Bilayer Ohmic Electrode Engineering in TaO_X ReRAM Devices

Godwin Paul, Tom Glint, Stephan Menzel, *Senior Member, IEEE*, and Vikas Rana

***Abstract*— TaO_X Redox-based Random Access Memory (ReRAM) is a strong candidate to replace existing memory technologies, offering low power consumption, high endurance, and long retention. However, reducing switching energy and enhancing switching uniformity are critical for practical applications. Previous efforts to improve switching uniformity have compromised device performance, leading to low On/Off ratio or high operating voltages. In this work, TaO_X ReRAM is engineered with bilayer ohmic electrodes (OE) and the switching mechanism for specific OE thicknesses is explored based on the switching behavior and material properties of OE. An optimized Ti(2 nm)/Ta(13 nm) bilayer OE ReRAM is presented with a reduced forming voltage, ∼11× (∼6×) faster mean SET (RESET) switching speeds, ∼6× lower mean switching energy and ∼10× lower resistance drift during long switching cycles compared to its single-layer OE counterpart, without degradation in other device performance metrics.**

***Index Terms*— Bilayer ReRAM, ReRAM engineering, resistance drift, switching mechanism, switching speed.**

I. Introduction

TaO_X switching oxide in ReRAMs enables fast low power switching [1], [2], [3], [4], and impressive endurance (10^{10} cycles) [5], [6] and retention (10 years at 85°C) [7], [8], due to its high oxygen solubility and low absolute Gibbs free energy for redox reactions. However, TaO_X devices have high forming voltage (V_{FORM}) and cycle-to-cycle variability, necessitating improvements to compete with commercial memory technologies [9], [10], [11]. Previous efforts to improve switching uniformity through interface engineering have led to trade-offs, such as a reduced R_{OFF}/R_{ON} ratio [12] or higher operating voltages [6], [13].

In Pt/TaO_X/Ta/Pt devices, based on the applied voltage, oxygen exchange with the Ta ohmic electrode (OE) forms or ruptures the oxygen vacancy (V_O) filament within the TaO_X switching oxide, enabling bipolar switching [9], [14]. The thickness and oxygen vacancy defect formation energy (E_{VO}) of the OE with respect to the TaO_X layer influence the forming and switching processes [14]. Hence, using multiple OE layers with optimized thicknesses and E_{VO} is a promising way to control filament evolution and improve switching properties.

Previous studies showed that adding Ti or Hf interlayers in Pt/TaO_X(10 nm)/Ta(100 nm)/Pt devices improved switching uniformity, attributed to comparable passive series resistances (R_S) of the oxidized interlayers [13], [15]. However, the impact of material properties and thicknesses of Interlayer-OE (I-OE, the OE in contact with TaO_X) and the top OE (Ta in this case) on switching characteristics and long-term switching stability of the TaO_X devices remain unexplored. These insights enables targeted device engineering, ensuring reliability and reproducibility of next-generation ReRAM technologies.

In this work, we studied various TaO_X-based bilayer OE devices. A modified switching mechanism is proposed for a specific device structure. Optimized bilayer OE devices show improved switching characteristics over single OE devices. This stack also reduces the high operation voltages previously observed in similar stacks with different layer thicknesses [13].

II. Device Fabrication and Measurement

In this study, $2 \times 2\ \mu m^2$ crossbar devices were fabricated on SiO_2(430 nm)/Si substrate. Firstly, the 5 nm-thick TiO_2 and 30 nm-thick Pt layers were deposited by PVD and patterned by photolithography and dry etching to form the bottom electrode. The 7 nm-thick TaO_X was then deposited by reactive sputtering in a process gas mixture of argon (77%) and oxygen (23%) with an RF power of 116 W at a chamber pressure of 2.3 x 10^{-2} mbar. Later, bilayer OE with different materials (Ti, Ta, or W) and a 30 nm-thick Pt top electrode (TE) were sequentially deposited by RF and DC sputtering, respectively, followed by patterning to complete ReRAM device fabrication.

The *I-V* characteristics and endurance were measured in a custom setup with a fast current compliance (I_{CC}) circuit, a waveform generator and an oscilloscope [16]. Switching kinetics were measured in *Keithley 4200A-SCS* parameter analyzer. All voltages shown are applied to the TE.

III. Results and Discussion

The SEM image and schematic of the bilayer OE devices are presented in Fig. 1(a). The devices are named xnmM_ynmN,

Received 20 May 2025; revised 18 June 2025; accepted 30 June 2025. Date of publication 2 July 2025; date of current version 4 September 2025. This work was supported in part by the Federal Ministry of Education and Research (BMBF), Germany, through the Project NEUROTEC under Grant 16ME0398K and Grant 16ME0399; and in part by the Jülich Aachen Research Alliance (JARA-[Fundamentals of Future Information Technology (FIT)]). The review of this letter was arranged by Editor B. Govoreanu. *(Corresponding author: Godwin Paul.)*

Godwin Paul, Tom Glint, and Vikas Rana are with PGI-10, Forschungszentrum Jülich GmbH, 52428 Jülich, Germany (e-mail: g.paul@fz-juelich.de).

Stephan Menzel is with PGI-7, Forschungszentrum Jülich GmbH, 52428 Jülich, Germany.

Digital Object Identifier 10.1109/LED.2025.3585469

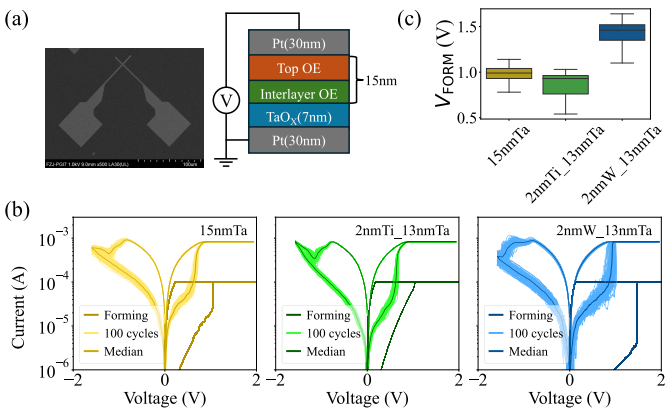

Fig. 1. (a) SEM image of fabricated device and schematic illustration of the standard bilayer OE stack. The total thickness of the bilayer OE is kept constant at 15 nm. (b) Typical DC *I-V* characteristics for forming and switching (100 cycles and median) of devices with different I-OE, measured under I_{CC} = 1.0 mA, $V_{SET\text{-}stop}$ = 2.0 V, and $V_{RESET\text{-}stop}$ = −1.6 V. (c) Statistical comparison of forming voltages across 96 devices for each I-OE configuration.

TABLE I
DEFECT FORMATION ENERGY (E_{VO}) OF METALS AND ACTIVATION ENERGY (E_A) FOR OXYGEN DIFFUSION IN METAL SUBOXIDES

Parameter	Ti	Ta	W
E_{VO} (eV) [14], [19], [20]	-0.6	0.1	1.4
E_a (eV) [21]–[23]	0.21	1.2 ± 0.1	1.3

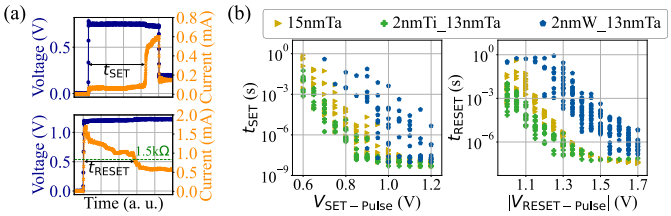

Fig. 2. (a) Method for extracting SET time (t_{SET}) and RESET time (t_{RESET}) from voltage pulse measurements without externally applied current compliance. The SET time is defined as the time between the voltage pulse reaching its maximum amplitude and the point of maximum current increase. The RESET time is defined as the time it takes for the resistance to exceed 1.5 kΩ. An R_{OFF}/R_{ON} ratio of more than 5× is maintained for all measurements. (b) t_{SET} and t_{RESET} values of devices are plotted against applied voltage pulse amplitudes.

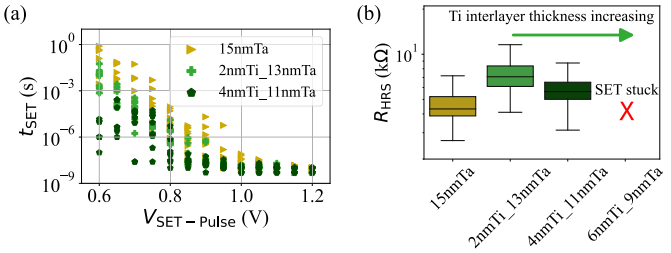

Fig. 3. (a) SET kinetics and (b) R_{HRS} for devices with different Ti I-OE thicknesses. R_{HRS} is extracted from 100 DC *I-V* sweep cycles of 10 devices from each OE combination, measured under I_{CC} = 1.0 mA, $V_{SET\text{-}stop}$ = 2.0 V, and $V_{RESET\text{-}stop}$ = −1.6 V.

where x is the deposited I-OE thickness, M is the I-OE material, y is the deposited top OE thickness and N the top OE material. The total thickness of the bilayer OE is maintained at 15 nm. For instance, a 2 nm-thick Ti layer corresponds to a 13 nm-thick Ta layer. Single OE devices are denoted 15nmM, where M is the OE material. Typical forming and switching characteristics of the devices of interest are shown in Fig. 1(b). Fig. 1(c) illustrates the impact of I-OE material on V_{FORM}. Compared to 15nmTa devices (median V_{FORM} = 0.99 V), 2nmTi_13nmTa devices exhibit lower V_{FORM} (0.93 V in median), while 2nmW_13nmTa devices show higher V_{FORM} (1.46 V in median). This is explained by E_{VO} of the I-OE material in Ta_2O_5 as listed in Table I. An I-OE with lower E_{VO} (Ti< Ta< W) will extract more oxygen from the TaO_X layer in pristine devices [14], making it more conductive. This leads to higher initial currents and more Joule heating when a voltage sweep is applied, which in turn enhances oxygen exchange rates. This finally triggers a self-accelerated thermal run-away, completing the electroforming process at lower voltages [17], [18].

The switching kinetics of the devices were investigated under varying voltage pulse amplitudes, as shown in Fig. 2(a). Both the SET and RESET processes occur faster in 2nmTi_13nmTa devices (∼11× faster mean t_{SET} at 0.8 V and ∼6× faster mean t_{RESET} at -1.25 V) and slower in 2nmW_13nmTa devices, compared to 15nmTa devices (Fig. 2(b)). Devices with an I-OE having a lower E_{VO} (Ti< Ta< W) exhibit a faster SET, consistent with [14], since the I-OE layer facilitates faster oxygen extraction. However, these devices also exhibit faster RESET, contrary to the E_{VO}-RESET speed relationship reported in [14], demanding further exploration. When the RESET voltage is applied to the TaO_X/Ta devices, a V_O gradient is created in the switching oxide, countered by a back-diffusion force. Gradual RESET occurs as repeated oxygen exchange with the OE reduces this force, lowering the vacancy concentration near the Pt electrode and decreasing the current [14]. Given that the I-OE layer (or 2 nm-thick Ta in 15nmTa devices) partially oxidizes, as seen for Ti in [13], and that the RESET process relies on continuous oxygen exchange, the interlayer suboxide likely acts as an oxygen diffusion layer during RESET. The activation energy for oxygen diffusion (E_a) from the literature follows the order TiO_X< TaO_X< WO_X (Table I), consistent with the observed RESET speed trend (2nmTi_13nmTa > 15nmTa > 2nmW_13nmTa). Since diffusion is believed to occur without the formation of point defects, this mechanism explains why the RESET speed is not related to the E_{VO} values of the I-OE layer.

t_{SET} and R_{HRS} are plotted for different Ti I-OE thicknesses in Fig. 3(a) and (b), respectively. The decrease in t_{SET} with increasing Ti I-OE thickness provides more evidence on E_{VO} driven SET process. The higher R_{HRS} in devices with a 2 nm-thick Ti I-OE compared to 15nmTa devices is explained by the lower E_a of TiO_X relative to TaO_X. However, with increasing I-OE thickness, R_{HRS} shifts from being governed by E_a of TiO_X to E_{VO} of Ti (devices are SET-stuck as in [14]), suggesting that OE functions as a diffusion layer near the switching oxide and as an oxygen reservoir layer further away.

R_{HRS} and t_{SET} of the devices are plotted for different top OEs in Fig. 4(a) and (b), respectively. Devices without (w/o) top OE remain SET-stuck, indicating that oxygen required

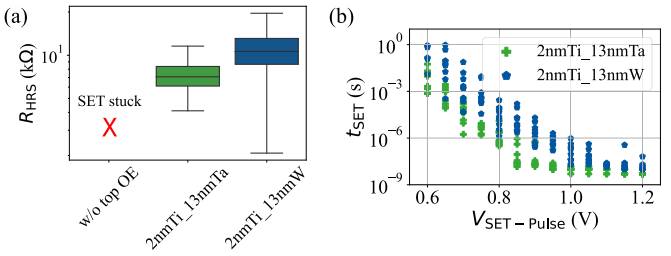

Fig. 4. (a) R_{HRS} and (b) SET kinetics for devices with different top OEs. The devices without (w/o) top OE are SET-stuck.

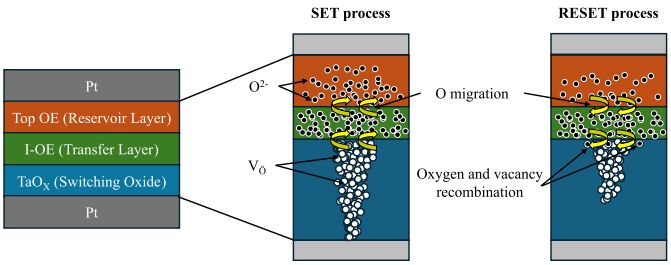

Fig. 5. Illustration of switching mechanism in 2 nm thick I-OE devices.

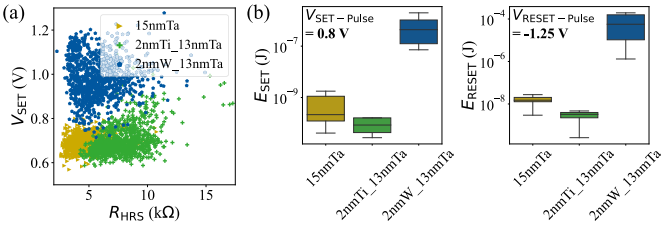

Fig. 6. (a) V_{SET} dependency on R_{HRS} plotted from DC *I-V* data. (b) SET and RESET energy extracted from pulse switching data in Fig. 2.

for RESET comes from the top OE, likely having migrated from the switching oxide during the forming or SET process. In addition, devices with W top OE show higher R_{HRS} and t_{SET} compared to those with Ta top OE, confirming that the general switching characteristics depend on E_{VO} of the top OE, even without direct contact with the switching oxide.

The observations indicate that in 2 nm-thick I-OE devices, the I-OE acts as a transfer layer facilitating oxygen exchange between the TaO_X layer and top OE (Fig. 5). The SET kinetics depend on E_{VO} and RESET kinetics on E_a of I-OE layer, while switching characteristics are influenced by the top OE's E_{VO}.

The V_{SET} vs R_{HRS} for devices with different I-OE is visualized in Fig. 6(a). Compared to 15nmTa devices, 2nmTi_13nmTa devices exhibit higher R_{HRS}, while 2nmW_13nmTa devices show higher V_{SET}. Consequently, the mean switching energy is reduced ∼6× in 2nmTi_13nmTa devices, while it increases in 2nmW_13nmTa devices, relative to the 15nmTa devices (Fig. 6(b)).

Fig. 7 shows cyclic endurance of TaO_X ReRAM with different I-OE layers over 10^7 *I-V* sweep cycles. The applied switching conditions (I_{CC} = 1.0 mA, $V_{RESET\text{-}stop}$ = −1.6 V) were optimized for all samples based on endurance measurements to ensure stable device performance and fair comparison across samples. The device stability is quantified by applying

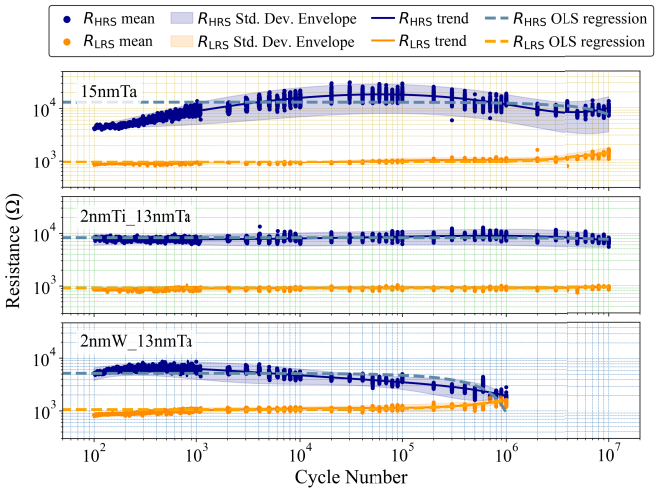

Fig. 7. Mean values of R_{HRS} and R_{LRS}, averaged over 10 devices each, plotted as a function of the number of DC *I–V* sweep cycles for different I-OE materials. Measurements were performed under I_{CC} = 1.0 mA, $V_{SET\text{-}stop}$ = 2.0 V, and $V_{RESET\text{-}stop}$ = −1.6 V.

TABLE II
OLS REGRESSION PARAMETERS FOR R_{HRS} AND R_{LRS} MEANS

Parameter	15nmTa	2nmTi_13nmTa	2nmW_13nmTa
R_{HRS} Slope	-5.72×10^{-7}	-6.18×10^{-8}	-4.20×10^{-6}
R_{LRS} Slope	4.30×10^{-8}	3.60×10^{-9}	5.35×10^{-7}

Ordinary Least Squares (OLS) regression to the mean values of R_{HRS} and R_{LRS} across cycles. Smaller mean slopes imply less resistance drift, with positive slopes showing an increase in resistance and negative slopes showing a decrease. The mean R_{HRS} and R_{LRS} of the 2nmTi_13nmTa devices show a ∼10× and ∼100× lower drift, compared to the 15nmTa and 2nmW_13nmTa devices, respectively (Table II). The endurance failure in the latter two devices is due to reduced R_{HRS} and increased R_{LRS}, which can be due to temperature-induced oxidation near the oxygen exchange interface (the I-OE layer in our case) [24]. Hence, the improved stability of the 2nmTi_13nmTa devices can be attributed to the low E_a of TiO_X compared to TaO_X and WO_X, potentially limiting the complete oxidation of Ti I-OE layer during prolonged oxygen exchange through this layer. Although the 2 nm-thick Ti I-OE improves long-term stability, a thicker Ti layer can be detrimental. According to the proposed mechanism, thicker Ti layer begins to act an oxygen reservoir, and its negative E_{VO} can hinder oxygen recovery during RESET, potentially causing RESET failure over repeated switching.

IV. CONCLUSION

In devices with 2 nm-thick I-OE, SET and RESET kinetics are governed by the E_{VO} and E_a of the I-OE, respectively, while the E_{VO} of the top OE influences the switching characteristics. Observations indicate that the I-OE facilitates oxygen exchange between the TaO_X layer and the top OE. Introducing a 2 nm-thick Ti I-OE into 15nmTa devices significantly enhances performance, highlighting bilayer OE engineering as a promising approach for advancing ReRAM technology.

REFERENCES

[1] A. C. Torrezan, J. P. Strachan, G. Medeiros-Ribeiro, and R. S. Williams, "Sub-nanosecond switching of a tantalum oxide memristor," *Nanotechnology*, vol. 22, no. 48, Dec. 2011, Art. no. 485203, doi: 10.1088/0957-4484/22/48/485203.

[2] C.-W. Hsu, C.-C. Wan, I.-T. Wang, M.-C. Chen, C.-L. Lo, Y.-J. Lee, W.-Y. Jang, C.-H. Lin, and T.-H. Hou, "3D vertical TaO_x/TiO_2 RRAM with over 10^3 self-rectifying ratio and sub-μA operating current," in *IEDM Tech. Dig.*, Dec. 2013, pp. 10.4.1–10.4.4, doi: 10.1109/IEDM.2013.6724601.

[3] W. Kim, B. Rösgen, T. Breuer, S. Menzel, D. Wouters, R. Waser, and V. Rana, "Nonlinearity analysis of TaOX redox-based RRAM," *Microelectronic Eng.*, vol. 154, pp. 38–41, Mar. 2016, doi: 10.1016/j.mee.2016.01.025.

[4] A. Prakash, D. Jana, and S. Maikap, "TaO_x -based resistive switching memories: Prospective and challenges," *Nanosc. Res. Lett.*, vol. 8, no. 1, pp. 1–17, Dec. 2013, doi: 10.1186/1556-276x-8-418.

[5] J. J. Yang, M.-X. Zhang, J. P. Strachan, F. Miao, M. D. Pickett, R. D. Kelley, G. Medeiros-Ribeiro, and R. S. Williams, "High switching endurance in TaOx memristive devices," *Appl. Phys. Lett.*, vol. 97, no. 23, Dec. 2010, Art. no. 232102, doi: 10.1063/1.3524521.

[6] M.-J. Lee, C. B. Lee, D. Lee, S. R. Lee, M. Chang, J. H. Hur, Y.-B. Kim, C.-J. Kim, D. H. Seo, S. Seo, U.-I. Chung, I.-K. Yoo, and K. Kim, "A fast, high-endurance and scalable non-volatile memory device made from asymmetric Ta_2O_{5-x}/TaO_{2-x} bilayer structures," *Nature Mater.*, vol. 10, no. 8, pp. 625–630, Aug. 2011, doi: 10.1038/nmat3070.

[7] Z. Wei, Y. Kanzawa, K. Arita, Y. Katoh, K. Kawai, S. Muraoka, S. Mitani, S. Fujii, K. Katayama, M. Iijima, T. Mikawa, T. Ninomiya, R. Miyanaga, Y. Kawashima, K. Tsuji, A. Himeno, T. Okada, R. Azuma, K. Shimakawa, H. Sugaya, T. Takagi, R. Yasuhara, K. Horiba, H. Kumigashira, and M. Oshima, "Highly reliable TaO_x ReRAM and direct evidence of redox reaction mechanism," in *IEDM Tech. Dig.*, Dec. 2008, pp. 1–4, doi: 10.1109/IEDM.2008.4796676.

[8] L. Goux, A. Fantini, Y. Y. Chen, A. Redolfi, R. Degraeve, and M. Jurczak, "Evidences of electrode-controlled retention properties in Ta_2O_5-based resistive-switching memory cells," *ECS Solid State Lett.*, vol. 3, no. 11, pp. Q79–Q81, Sep. 2014, doi: 10.1149/2.0011412ssl.

[9] R. Waser, R. Dittmann, G. Staikov, and K. Szot, "Redox-based resistive switching memories–nanoionic mechanisms, prospects, and challenges," *Adv. Mater.*, vol. 21, nos. 25–26, pp. 2632–2663, Jul. 2009, doi: 10.1002/adma.200900375.

[10] F. Zahoor, T. Z. Azni Zulkifli, and F. A. Khanday, "Resistive random access memory (RRAM): An overview of materials, switching mechanism, performance, multilevel cell (MLC) storage, modeling, and applications," *Nanosc. Res. Lett.*, vol. 15, no. 1, pp. 1–26, Dec. 2020, doi: 10.1186/s11671-020-03299-9.

[11] H.-S. P. Wong, H.-Y. Lee, S. Yu, Y.-S. Chen, Y. Wu, P.-S. Chen, B. Lee, F. T. Chen, and M.-J. Tsai, "Metal–oxide RRAM," *Proc. IEEE*, vol. 100, no. 6, pp. 1951–1970, Jun. 2012.

[12] Y. B. Zhu, K. Zheng, X. Wu, and L. K. Ang, "Enhanced stability of filament-type resistive switching by interface engineering," *Sci. Rep.*, vol. 7, no. 1, p. 43664, May 2017, doi: 10.1038/srep43664.

[13] X. Y. Li, X. L. Shao, Y. C. Wang, H. Jiang, C. S. Hwang, and J. S. Zhao, "Thin TiO_x layer as a voltage divider layer located at the quasi-ohmic junction in the $Pt/Ta_2O_5/Ta$ resistance switching memory," *Nanoscale*, vol. 9, no. 6, pp. 2358–2368, 2017, doi: 10.1039/c6nr08470b.

[14] W. Kim, S. Menzel, D. J. Wouters, Y. Guo, J. Robertson, B. Roesgen, R. Waser, and V. Rana, "Impact of oxygen exchange reaction at the ohmic interface in Ta_2O_5-based ReRAM devices," *Nanoscale*, vol. 8, no. 41, pp. 17774–17781, 2016, doi: 10.1039/c6nr03810g.

[15] Y. Wang, Y. Yan, C. Wang, Y. Chen, J. Li, J. Zhao, and C. S. Hwang, "Controlling the thin interfacial buffer layer for improving the reliability of the $Ta/Ta_2O_5/Pt$ resistive switching memory," *Appl. Phys. Lett.*, vol. 113, no. 7, Aug. 2018, Art. no. 072902, doi: 10.1063/1.5040430.

[16] T. Hennen, E. Wichmann, A. Elias, J. Lille, O. Mosendz, R. Waser, D. J. Wouters, and D. Bedau, "Current-limiting amplifier for high speed measurement of resistive switching data," *Rev. Sci. Instrum.*, vol. 92, no. 5, May 2021, Art. no. 054701, doi: 10.1063/5.0047571.

[17] R. Dittmann, S. Menzel, and R. Waser, "Nanoionic memristive phenomena in metal oxides: The valence change mechanism," *Adv. Phys.*, vol. 70, no. 2, pp. 155–349, Apr. 2021, doi: 10.1080/00018732.2022.2084006.

[18] A. Marchewka, R. Waser, and S. Menzel, "Physical modeling of the electroforming process in resistive-switching devices," in *Proc. Int. Conf. Simul. Semiconductor Processes Devices (SISPAD)*, Sep. 2017, pp. 133–136, doi: 10.23919/SISPAD.2017.8085282.

[19] Y. Guo and J. Robertson, "Materials selection for oxide-based resistive random access memories," *Appl. Phys. Lett.*, vol. 105, no. 22, Dec. 2014, Art. no. 223516, doi: 10.1063/1.4903470.

[20] Y. Guo and J. Robertson, "Origin of the high work function and high conductivity of MoO_3," *Appl. Phys. Lett.*, vol. 105, no. 22, Dec. 2014, Art. no. 222110, doi: 10.1063/1.4903538.

[21] S. Y. Sarvadii, A. K. Gatin, V. A. Kharitonov, N. V. Dokhlikova, S. A. Ozerin, M. V. Grishin, and B. R. Shub, "Oxidation of thin titanium films: Determination of the chemical composition of the oxide and the oxygen diffusion factor," *Crystals*, vol. 10, no. 2, p. 117, Feb. 2020, doi: 10.3390/cryst10020117.

[22] R. Nakamura, T. Toda, S. Tsukui, M. Tane, M. Ishimaru, T. Suzuki, and H. Nakajima, "Diffusion of oxygen in amorphous Al_2O_3, Ta_2O_5, and Nb_2O_5," *J. Appl. Phys.*, vol. 116, no. 3, Jul. 2014, Art. no. 033504, doi: 10.1063/1.4889800.

[23] V. K. Sikka and C. J. Rosa, "The oxidation kinetics of tungsten and the determination of oxygen diffusion coefficient in tungsten trioxide," *Corrosion Sci.*, vol. 20, nos. 11–12, pp. 1201–1219, Jan. 1980, doi: 10.1016/0010-938x(80)90092-x.

[24] B. Chen, Y. Lu, B. Gao, Y. H. Fu, F. F. Zhang, P. Huang, Y. S. Chen, L. F. Liu, X. Y. Liu, J. F. Kang, Y. Y. Wang, Z. Fang, H. Y. Yu, X. Li, X. P. Wang, N. Singh, G. Q. Lo, and D. L. Kwong, "Physical mechanisms of endurance degradation in TMO-RRAM," in *IEDM Tech. Dig.*, Dec. 2011, pp. 12.3.1–12.3.4, doi: 10.1109/IEDM.2011.6131539.